RSC Advances

ROYAL SOCIETY OF CHEMISTRY

www.rsc.org/advances

Insertion of isatin molecule into the nanostructure of palygorskite

Wei Zhou，Hong Liu， Tingting Xu，Yeling Jin， Shijie Ding，Jing Chen*

Faculty of Life Science & Chemical Engineering, Key Laboratory for Palygorskite Science and Applied Technology of Jiangsu, Huaiyin Institute of Technology, Jiangsu Province, Huaian, 223003, P. R. China

Abstract: Palygorskite has unique grooves and channels nanostructure to protect the inserted molecule from ruin, and Maya blue is a perfect example. In this paper, a new hybrid pigment prepared by inserting isatin into palygorskite was synthesized and analyzed. The hybrid could retain its vivid color even after being boiled for 5 h in 30 % H_2O_2 aqueous solution. Protected by palygorskite, 59 % isatin successfully survived 72 h $CHCl_3$ Soxhlet extraction of the hybrid. Ultraviolet-near infrared spectroscopy (UV-NIR) and Fourier transform infrared spectroscopy (FT-IR) indicated that the conjugate plan of isatin might be distorted when inserted to palygorskite, just like indigo did in Maya blue. X-ray diffraction analysis (XRD) and high-resolution transmission electron microscopy (HRTEM) pointed out that palygorskite exhibited a certain degree of lattice distortion after hybridization. Thermal gravity and differential thermal gravity analysis (TG-DTG) showed further that the small-size isatin could go deeper into the channels of palygorskite and block the channel entrance better than indigo did in Maya blue. All the analyses indicated that isatin inserted deeply into the clay, and the insertion is much deeper than that of

* Corresponding author. Tel.: +86 517 83591044; fax: +86 517 83591190.
E-mail address: chenjing6910@163.com (D. Chen).

indigo.

Key Words：chemical stability；hybrid；isatin；palygorskite

Introduction

Maya blue is a famous organo-clay hybrid pigment produced by ancient Mayas, which retains its vivid color against wind and rain erosion over thousands of years.[1] Although the primitive preparation method of Maya blue is unknown, it is confirmed by modern analytical technique that Maya blue consists of two main ingredients: indigo (Fig.1) (which is obtained from the leaves of the *añil* plant, *Indigofera suffruticosa*) and palygorskite (which is found in the Yucatán Peninsula).[2,3] Palygorskite is a kind of natural fibrous clay (Fig. 1), its idealized structural formula is $Si_8(Mg_2Al_2)O_{20}(OH)_2(OH_2)_4 \cdot 4H_2O$).[4-6] Most of the present studied samples were prepared by crushing the mixture of palygorskite and indigo, and then treated with moderate heat treatment.[1,3,7-12]

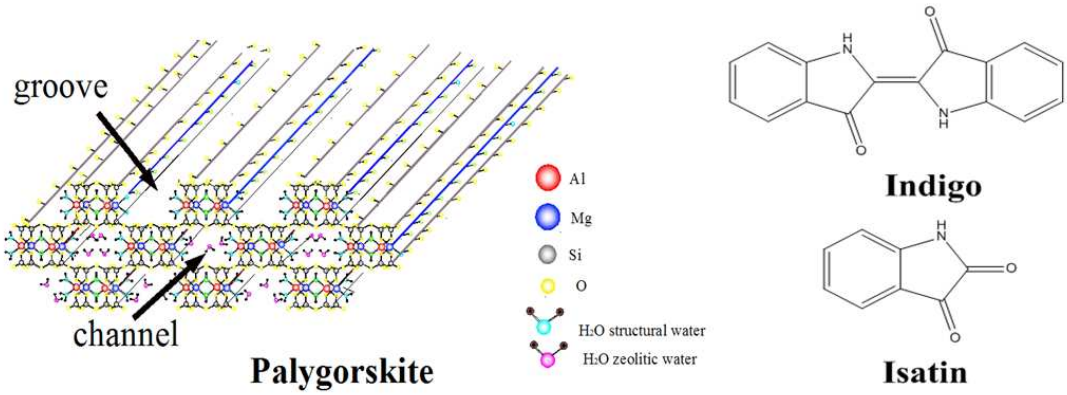

Fig. 1. The structure of palygorskite, indigo and isatin molecule.

Gettens et al., tested many survival samples and found that Maya blue had unprecedented stability against violent attack of acids, alkalis and biodegradation.[2]

The academia have reached agreement on that the unique grooves and channels structure of palygorskite provided perfect protection to the indigo molecules.[3] However, the nature of the indigo-palygorskite association was under long time controversy. Van Olphen suggested that the indigo molecules were too large to enter the channels of the clay, thus its beautiful color was due to the indigo adsorbed by the external grooves of palygorskite.[3] Polette-Niewold et al., supported this viewpoint through multiple analytical techniques and density functional theory calculations.[1] Considering the dimmesion of the channel and the size of indigo molecules, Kleber et al., pointed out that the penetration of indigo into the channels could not be excluded.[7] Based on data collected by synchrotron radiation, Chiari et al., proved that indigo could fit into the channel of palygorskite without steric impediment by molecular modeling.[13] Fois et al., elucidated that the indigo molecules did get into the channels by classical molecular dynamic simulations, which contributed to understand why Maya blue was exceptionally stable in hot concentrated acids.[14] TG-DTG, solid-state nuclear magnetic resonance (SSNMR) and synchrotron XRD were introduced to experimentally prove that the indigo molecules blocked the endings of palygorskite channels.[15] Sánchez del Río et al., agreed that there was a possible partial penetration when indigo blocked on the channel entrance, with synchrotron powder diffraction and Raman spectroscopy as the main analyze methods.[16] The bonding mode between indigo and palygorskite is another research subject, and there are three main points of view: ①the hydrogen bonds are between indigo and silanol group of the clay;[15] ②the hydrogen bonds are between indigo and coordinated water or some zeolite water inside the channels of the clay;[13,14,17] ③

indigo molecules bond to the octahedral metal ion of the clay directly.[18,19] Besides, Van der Waals force between indigo and palygorskite was also significant in stabilizing Maya blue.[14,20]

The research of Maya blue has inspired many analogues syntheses and characterizations. Van Olphen reported that indigo could be complex with plate-like structure clay, such as kaolinite, nontronite, Wyoming bentonite, and mordenite (cage-type zeolite).[3] The complexes have similar outlook to Maya blue but poor chemical stability. Sepiolite, homologous to palygorskite, could form a relatively stable composite with indigo, but still weaker than that of palygorskite.[21-23] Therefore, the channel structure seems to be essential for achieving stable pigments,[3] and the size of indigo molecule matches the palygorskite channel perfectly, resulting in the greatest stability.[21] Giustetto et al., proposed that H-bonds could only form on one side in sepiolite (whose channels were wider than those of palygorskite), whereas both sides were involved for palygorskite.[22,23] In addition, natural zeolite and silicalite were also used to explore the preparation of Maya blue analogues.[24,25] Zhang et al., synthesized a Maya blue-like photocatalyst with palygorskite and Eosin Y. They found that the hybrid was very useful for building a novel efficient hydrogen evolution system.[26] Yasarawan et al., found that indigo molecules ordered inside the sepiolite channels along its long axes, thus, the hybrid would show prominent dichroism, which made sense for the dye-doped thermotropic liquid crystals.[27] Photosensitive organic dyes have been widely used in solar cell,[28] light storage

device[29] and optical switch[30]etc. However, generally speaking, organic pigments could not bear long-term harsh environments. If the stability of these photosensitive dyes could be improved or a good micro-environment could be given to the dyes, related commercial applications would be promoted greatly. Maya blue is an extremely valuable reference, and some advanced work should base on it. This paper investigated a hybrid pigment of isatin (Fig. 1), a small dye molecule which was half of indigo not only in volume but also in structure, inserting into palygorskite. The study focused on the structure and performance character of the hybrid in order to further understand the formation mechanism of Maya blue and provide useful information for preparing other promising hybrid pigments.

Experimental

2.1 Materials

Palygorskite was obtained from Xuyi Zhongyuan Minerals Co. Ltd (China), the chemical compositions (wt.%) of the used palygorskite in our experiment was: SiO_2, 65.1; MgO, 16.4; Al_2O_3, 9.35; Fe_2O_3, 5.33; CaO, 1.23 and other small amounts of K_2O, TiO_2, P_2O_5, MnO etc. Isatin was purchased from Shanghai Jingchun reagent Co. Ltd (China). The other reagents were all analytically pure, used without further purification. All the aqueous solutions were prepared with ultrahigh purity water from a milli-Q purification system (Milli-Q Direct 8, Merck Millipore, USA)

2.2 Preparation of the hybrid

Palygorskite was milled and collected through 200 mesh sieve (<74 μm) before experiment. The clay was well mixed with 10 % (mass) isatin, followed with 48 h heat treatment at 130 ^{o}C. The product was the hybrid pigment of isatin and palygorskite. Soxhlet extraction was introduced to clear the unbounded isatin molecules via $CHCl_3$ extracting (more than 72 hour) until no dissolved isatin was detected by UV-Vis spectra.

2.3 Characterization

FT-IR spectra of the samples were recorded by a FT-IR spectrometer (Nicolet 5700, Thermo Electron Co., USA) with KBr as background. The resolution was 4 cm^{-1} and each spectrum was an average of 32 scans from 4000 to 400 cm^{-1}. X-ray power diffractometer (D8Discover, Bruker AXS, Germany) was used to get XRD patterns, using Cu-Kα radiation (λ=0.15406 nm, 40 kV, 40 mA), and scanned from 5 to 45° (2θ) with 0.5 sec·$step^{-1}$. Element analysis was done on an element analyzer (Vario III, Elementar, Germany) under He atmosphere, each value was the mean of three replicates with error less than 0.1 %. Brunauer-Emmett-Teller (BET) surface area and micropore measurements were performed on a Micromeritics TriStar II 3020 (Micromeritics Instrument Co., USA) at 77K. BET surface areas were estimated by the BET method, micropore surface areas, external surface areas and micropore volumes were obtained by the t-plot method. The samples were outgassed for 1.5 h at 105 °C in N_2 atmosphere before the measurements. UV-NIR spectra were collected by a Shimadzu UV3600 spectrophotometer (UV-3600, Shimadzu, Japan) in the 240-2400 nm range by diffuse reflectance mode with $BaSO_4$ as background. UV-Vis spectra were recorded by a spectrophotometer (UV-2401PC, Shimadzu,

Japan) in the 200-500 nm range, the concentration of the suspension was 0.1‰. TG-DTG analysis was achieved by a thermal analyzer (STA409PC, Netzsch Co., Germany) in N_2 atmosphere at 5 $^{o}C \cdot min^{-1}$ programming rate. TEM and HRTEM images were obtained using a high-resolution transmission electron microscope (Tecnai G^2 F20 S-Twin FEI USA) with a point resolution of 0.24 nm running at 200 KeV. All samples were analyzed without extracting treatment except Element analysis.

Considering the environment of dye application, antioxidant property was selected to evaluate the chemical stability of the samples. The treatment was boiling the samples in 30 % H_2O_2 solution for 5 h.

Results and discussion

3.1 Element analysis

Harsher Soxhlet extraction was a powerful dissolution, which could clean out the unbounded dye molecules from the hybrid, and the remained dye must be protected by palygorskite. In this experiment, unbounded dye molecules were cleaned out from the hybrid by Harsher Soxhlet extraction with $CHCl_3$.[27] Compared with 0.076 % isatin residue for the simple mixture contained 10 % isatin, 5.9 % isatin was preserved for that after 48 h heat treatment. This result showed that the heat treatment was crucial to prepare a stable isatin-palygorskite hybrid, and simple mixing could not obtain good hybridization. This was consistent with the former hybrid conclusion of indigo with palygorskite.[3] The saturated doping contents of isatin to palygorskite was close to 6.5 wt% in our experiments (relative data would be shown in later report), but the theoretical value should be about 14 % if isatin

molecules spreaded on the surface of palygorsktie in a mono-molecular adsorption way. The result indicated that isatin should have special reactive positions to the clay.

3.2 BET Analysis

Table 1. BET surface area analysis by N_2 adsorption-desorption experiments of palygorskite and the hybrid.

	palygorskite	palygorskite after heating	hybrid
BET Surface Area (m^2/g)	164.8	180.6	61.9
Micropore area (m^2/g)	81.1	88.7	13.7
External Surface Area (m^2/g)	83.6	91.9	48.2
Micropore volume (mm^3/g)	37.3	40.6	5.7

The BET surface areas, micropore area, external surface area and micropore volume of the palygorskite increased after heating at 130 °C for 48 h. The increased surface area was mainly resulted from the loss of adsorbed water and zeolite water in the grooves and channels.[27] For the hybrid, all the tested data decreased, which should be due to the surface occupation by the isatin molecules, especially on the outside grooves of palygorskite.

3.3 UV-NIR and UV-Vis spectra analyses

There were two main characteristic diffraction bands of palygorskite (Fig. 2a). The one at 1426 nm was attributed to the first overtone of hydroxyl stretching mode, and the 1918 nm band was attributed to the combination of water stretching vibration and deformation modes.[31,32] For isatin (Fig. 2b), the band at 302 nm and 520 nm was due to the $\pi \rightarrow \pi^*$ and $n \rightarrow \pi^*$ electronic transition, respectively,[32,33] while the peak at 1666 nm was assigned to the first overtone of the C-H stretching vibration of benzene ring.[34] The bands at 302 and 520 nm of isatin shifted to 319 and 490 nm for

that of the hybrid respectively (Fig. 2c), meanwhile, the absorption bands were obviously narrowed down. Compared with the pure dye, palygorskite provided isatin molecules a higher polar micro-environment which prevented the aggregation of the dye molecules, so the broad absorption band of pure isatin narrowed down for the hybrid. This observation was analogous to indigo in Maya blue.[35,36] The bands of hydroxyl and water had some intensity loss and slight red-shift for the hybrid (Fig. 2c). This change should be due to the removing of water and deep insertion of isatin into the clay during heat treatment which changed the chemical environment of hydroxyl and coordinated water.

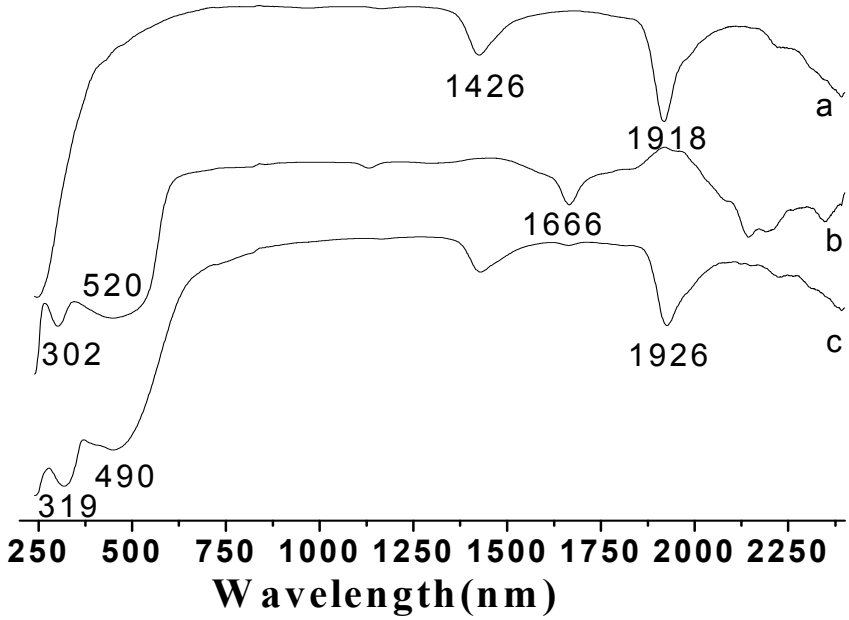

Fig. 2. UV- NIR reflectance spectra of palygorskite (a), isatin (b), the hybrid pigment purified by $CHCl_3$ (c).

Isatin had three absorption bands at 207 nm, 241 nm and 305 nm (Fig. 3a). The band at 241 nm was a strong peak due to the conjugation of carbonyl group and benzene ring.[32,33] Palygorskite had only one peak around 200 nm (Fig. 3c). As for the

hybrid (Fig. 3b), the sample color became darker than the unheated one, and the characteristic peaks were remained but shift to the red significantly. Fig. 3 indicated that the dye molecular structure was not destroyed but the chromophore was affected.

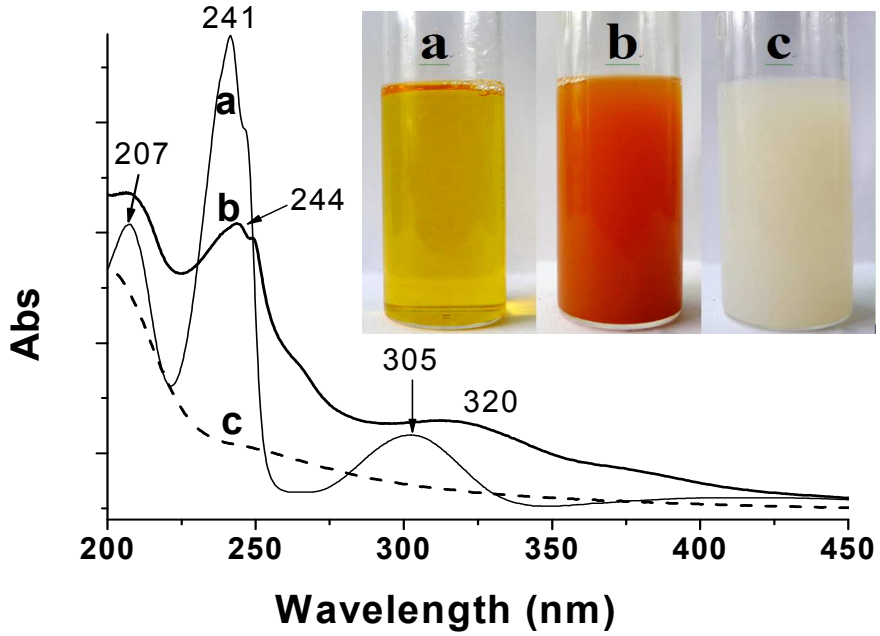

Fig. 3. UV-visible transmittance spectra of isatin (a), the hybrid (b), palygorskite (c).

3.4 FT-IR spectra analysis

Fig. 4a showed FT-IR spectrum of palygorskite. The stretching vibration of Si-OH was at 3736 cm^{-1}.[36] The hydroxyl stretching vibrations of molecular water coordinated to octahedral cation appeared at 3614 and 3576 cm^{-1}.[31,37-39] The absorption peaks at 3417 and 3253 cm^{-1} were attributed to the stretching vibration of free water.[31,39] The peak at 1658 cm^{-1} and the shoulder peak at 1643 cm^{-1} could be assigned to the bending vibration of zeolitic water and adsorbed water respectively.[31,37] There were four main peaks from1200 to 900 cm^{-1} originated from tetrahedral Si-O and Si-O-Si stretching vibrations.[5,6,38] The FT-IR spectrum of isatin

(Fig. 4c) showed the stretching vibration of N-H at 3446 cm^{-1}, characteristic absorption band of aromatic amine at 3193 cm^{-1}, stretching vibration of C=O at 1726 cm^{-1}, aromatic vibrations at 1612 cm^{-1}, plane bending vibration of C-H at 1463 cm^{-1}, and the asymmetric stretching vibration of C-N at 1331 cm^{-1}.[8,32]

As for the hybrid (Fig.4b), there were obvious blue shift of the bands of isatin at 1726, 1612, 1463 and 1331 cm^{-1}. This change should be attributed to the isatin micro-environment change after its insertion into palygorskite. Witke et al., pointed out that the deformation of indigo molecule might occur during the formation of Maya blue and the same was probably true for isatin.[40] The 1658 cm^{-1} band shrinked to disappear or was covered by the peak of isatin since heat treatment removed adsorbed water and zeolitic water. Compared with the shrinking of water band (3417 cm^{-1}), the Si-OH band (3736 cm^{-1}) seamed to be unaffected, while the coordinated water bands (3614, 3576 cm^{-1}) decreased more greatly. This result indicated that the insertion of isatin had a great influence on the coordinated OH_2, and the reaction sites should be more close to the octahedral cations of palygorskite.

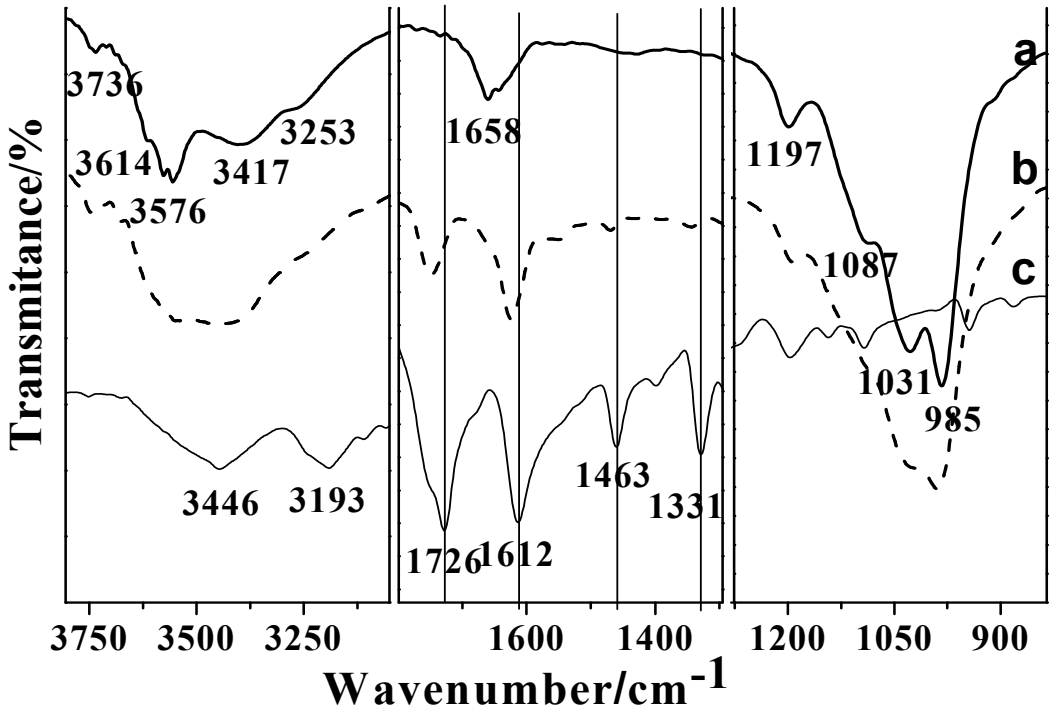

Fig. 4. FT-IR spectra of palygorskite (a), the hybrid (b), isatin(c).

3.5 TG-DTG analyses

The sample of palygorskite had four typical mass loss steps in its TG curve (Fig. 5a). These thermal behavior of palygorskite was similar to the previous works.[5,9,41] The first mass loss (12.5 %) was due to the loss of interparticle adsorbed water and zeolitic water with the maximum rate at 75 ^{o}C and 109 ^{o}C (shown on its DTG) respectively. The second mass loss (4.2 %) was at about 260 ^{o}C, which was assigned to the loss of first structural water. The third mass loss (5.2 %) was due to the loss of the second structural water, reaching its maximum rate at 441 ^{o}C. The fourth mass loss (2.1%) could be due to the dehydroxylation of the OH units about 657 ^{o}C. Isatin began its degradation from 204 ^{o}C and reached its largest mass loss at 306 ^{o}C (Fig. 5b).

Comparing Fig. 5a with Fig. 5c, though much smaller than that of palygorskite

(12.5%), the first mass loss of the hybrid was still obviously exist (4.85%). There were two possible situations for this phenomenon: a part of zeolitic water was remained in the channels, or the clay was rehydrated on its surface. Since the first structural water for the hybrid was almost negligible, rehydration was more preferable. It was very different from Maya blue that isatin-polygorskite hybrid had nearly no first structural water, which suggested isatin had perfectly sealing capacity to the channel than indigo did. The reason should be due to structural and dimensional differences between the two dyes. The indigo molecules were too bulky to seal the channels perfectly, so large hole had to be left, as a result, zeolitic water and the first structural water could be easier to recover for indigo-polygorskite hybrid. On the contrary, the small-size isatin could go deep into the channels, and constructed better blocks to the entry. The blocks restricted water molecule went back into the channels after hybridization.

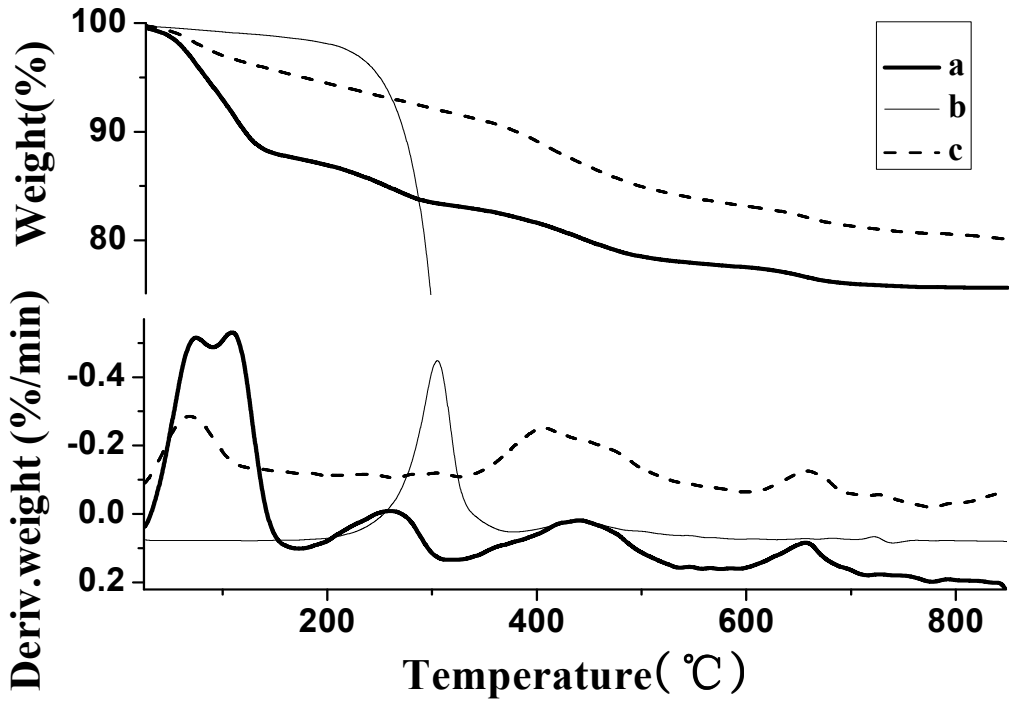

Fig. 5. TG-DTG curves of palygorskite (a), isatin (b), the hybrid (c).

3.6 XRD investigation

The sample clay had a typical XRD stratum of palygorskite with high purity (Fig. 6b). The sharp diffractions at 8.33°, 13.60°, 16.33°, 19.83° and 35.25° were attributed to the characteristic diffractions of palygorskite.

The hybrid (Fig. 6a) had similar diffractions as palygorskite, slight but measurable changes could still be observed. (110) diffractions shifted 0.04° to higher degree with 0.051 Å interplanner distance decrement, and (200) was 0.1° (0.047 Å), while the (130), (040) and (161) diffractions shifted to the lower degree with 0.04 ° (0.013 Å)、0.07° (0.016 Å) and 0.09° (0.006 Å) interplanner distance increment, respectively. The (002) diffraction almost disappeared after hybridization. The above XRD analysis indicated that the insertion of isatin into palygorskite must along certain direction in order to match its crystal structure. As a result, the palygorskite crystal lattice distorted to some extent.

Compared with Fig. 6c, isatin diffractions could not be observed in the XRD patterns of the hybrid (Fig. 6a), though the dye content amounted to 10 %. The heat treatment dispersed isatin molecule across the exterior surface of the clay, and inserted isatin into the channel of palygorskite. This process changed isatin from crystal state to a nearly mono-disperse amorphous state, hence its crystal characteristic patterns disappeared form the XRD patterns of the hybrid, just like indigo did in Maya blue.[1]

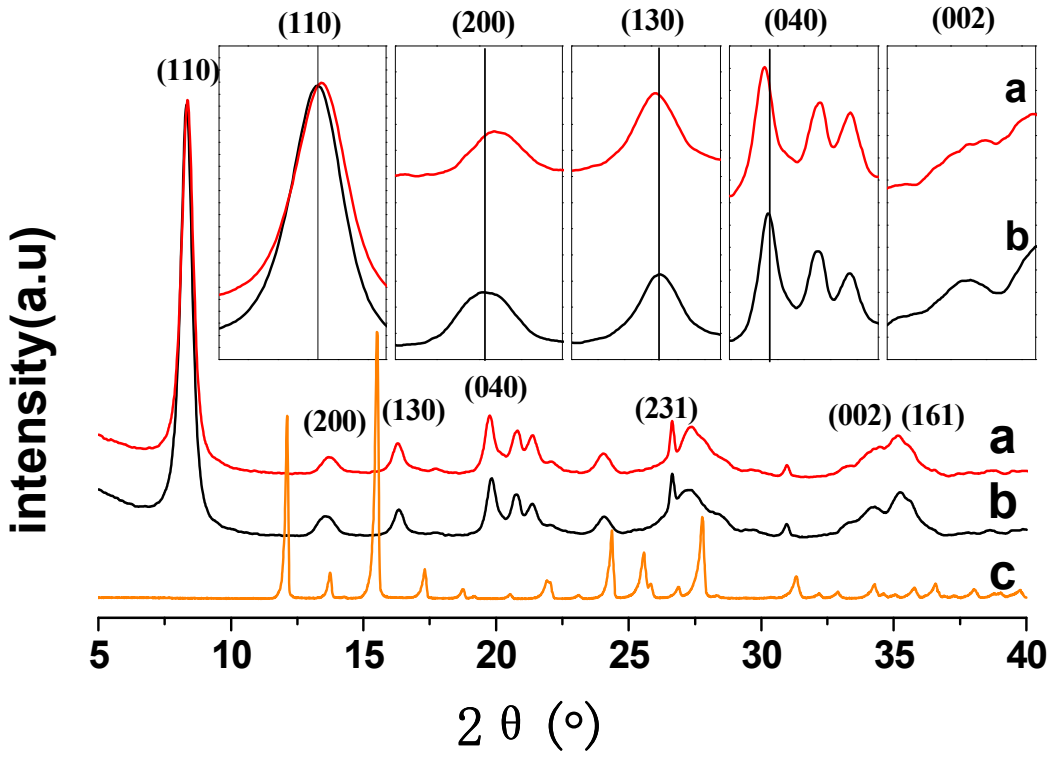

Fig. 6. XRD patterns of the hybrid (a), palygorskite (b), isatin (c).

3.7 HRTEM

The hybrid had very slight change from the clay (even in SEM analysis), so we applied HRTEM to analyze the change of morphology. Micrographs of palygorskite and the hybrid obtained from (110) direction were displayed in Fig. 7, showing well-defined parallel strips. This result illustrated that the reaction didn't destroy the structure of palygorskite. However, the strip distance of isatin-palygorskite hybrid (10.562 Å) became smaller compared to that of palygorskite (10.661 Å). It further supported that the insertion of the isatin molecules into the clay was along certain direction, resulting in a slight lattice distortion of palygorskite.

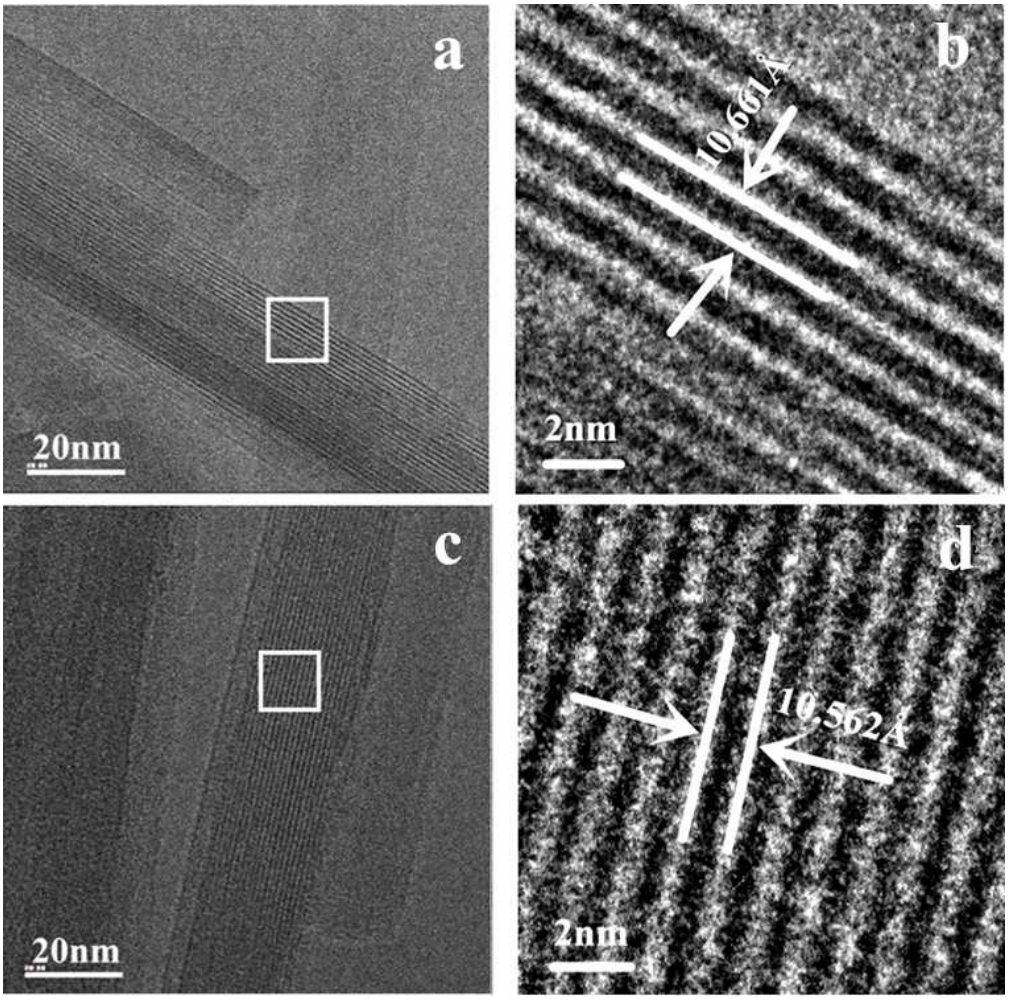

Fig. 7. TEM and HRTEM images of the palygorskite (a、b) and the hybrid (c、d).

3.8 Inoxidability

The remarkable resistance of Maya blue to chemical degradation was due to the protection of palygorskite.[3,7,13,14,22] Thus, the isatin-palygorskite hybrid should have similar chemical stability. The inoxidability of the hybrid was tested by 30% H_2O_2 refluxing for 5h. The bands of isatin disappeared completely after oxidation (Fig. 8d), the sample prepared by simple mixture only had a very weak band around 245 nm (Fig. 8c), while the hybrid synthesized by heat treatment (Fig. 8b) showed well characteristic band of isatin after oxidation treatment, though slightly weakened. The

inoxidability expreriment provided reasonable evidence that heat treatment was the key for the hybrid against erosion, and isatin inserted into the channels of palygorskite could gain good protection

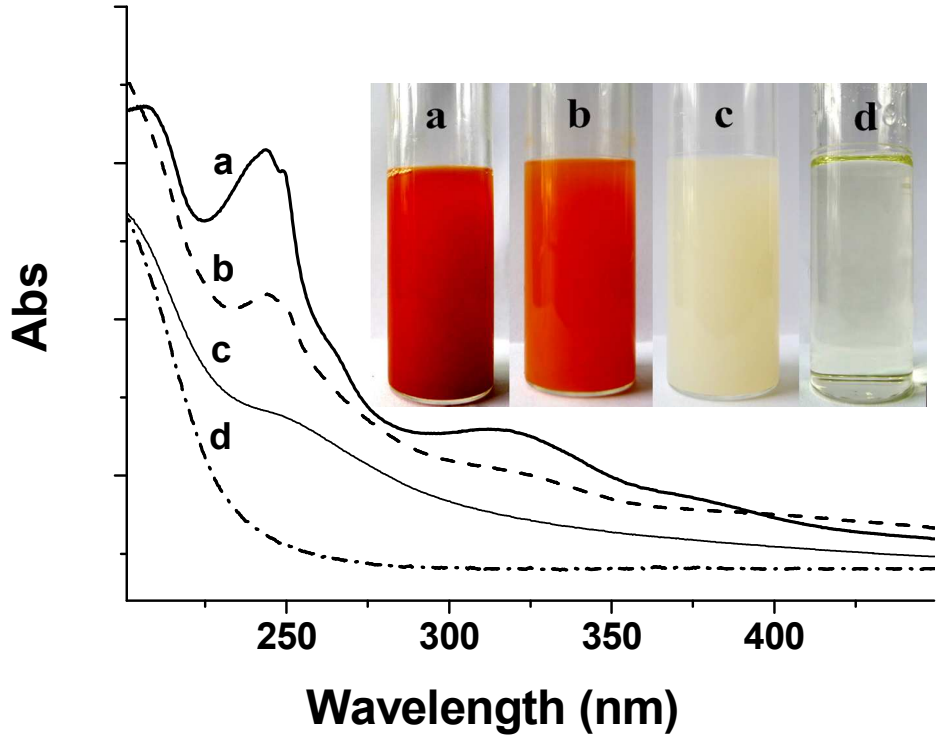

Fig. 8. UV-visible transmittance spectra of the hybrid (a), the hybrid after oxidization (b), the simple mixture after oxidization (c), isatin after oxidization (d).

4 、Conclusions

Isatin, a small dye which was half of indigo in both volume and structure, does have much deeper insertion to the palygorskite. This high degree hybridization brings some new experimental information that has not been found in Maya blue yet: for example, the obvious peak shift in XRD patterns, and a direct HRTEM evidence on the lattice distortion of the clay. FT-IR spectrua show that the conjugate plan of istain was distorted to some extent during the insertion. Moreover, isatin showed better sealing capability to the channel entry of palygorskite than indigo did, which

306 could be decued from the TG-DTG analysis.

307

308 **Acknowledgment**

309 The authors are grateful to National Natural Science Foundation of China
310 (51174096 and 21174046) for financial support of this work.

311

312 **References**

313 1. L. A. Polette-Niewold, F. S. Manciu, B. Torres, M. Alvarado, Jr. and R.
314 R. Chianelli, *J. Inorganic Biochem.*, 2007, **101**, 1958-1973.
315 2. R. J. Gettens, *Am. Antiquity*, 1962, 557-564.
316 3. H. Van Olphen, *Science*, 1966, **154**, 645-646.
317 4. E. García-Romero, M. S. Barrios, M. A. B. Revuelta, *Clay Clay Miner,*
318 2004, **52**, 484-494.
319 5. W. Yan, D. Liu, D. Tan, P. Yuan and M. Chen, *Spectrochim. Acta, Part A,*
320 2012, **97**, 1052-1057.
321 6. W. Yan, P. Yuan, M. Chen, L. Wang and D. Liu, *Appl. Surf. Sci.*, 2013,
322 **265**, 585-590.
323 7. R. Kleber, Masschelein-Kleiner,L.,Thissen,J., *Stud. Conserv.*, 1967, **12**,
324 41-55.
325 8. F. S. Manciu, L. Reza, L. A. Polette, B. Torres and R. R. Chianelli, *J.*
326 *Raman Spectrosc.*, 2007, **38**, 1193-1198.
327 9. R. Giustetto, F. X. Llabrés i Xamena, G. Ricchiardi, S. Bordiga, A.
328 Damin, R. Gobetto and M. R. Chierotti, *J. Phys. Chem. B*, 2005, **109**,
329 19360-19368.
330 10.C. Reyes-Valerio, *Siglo XXI Ed*,1993,157.
331 11. D. E. Arnold, J. R. Branden, P. R. Williams,G. M. Feinman and J. P.
332 Brown, *Antiquity,* 2008, **82**, 151-164.
333 12. E. Lima, A. Guzmán, M. Vera, J. L. Rivera and J. Fraissard, *J. Phys.*
334 *Chem. C,* 2012,**7**,4556-4563.
335 13. G. Chiari, R. Giustetto and G. Ricchiardi, *Eur. J. Mineral.*, 2003, **15**,
336 21-33.
337 14. E. Fois, A. Gamba and A. Tilocca, *Microporous Mesoporous Mater.*,
338 2003, **57**, 263-272.
339 15. B. Hubbard, W. Kuang, A. Moser, G. A. Facey and C. Detellier, *Clays*
340 *Clay Miner.* 2003, **51**, 318-326.
341 16. M. Sánchez del Río, E. Boccaleri, M. Milanesio, G. Croce, W. Beek, C.

Tsiantos, G. D. Chyssikos, V. Gionis, G. H. Kacandes, M. Suárez and E. García-Romero, *J. Mater. Sci.*, 2009, **44**, 5524-5536.

17. R. R. Chianelli, M. Perez De la Rosa, G. Meitzner, M. Siadati, G. Berhault, A. Mehta, J. Pople, S. Fuentes, G. Alonzo-Nunez and L. A. Polette, *J. Synchrotron Radiat.,* 2005, **12**, 129-134.

18. G. Chiari, R. Giustetto, J. Druzik, E. Doehne and G. Ricchiardi, *Appl. Phys. A: Mater. Sci. Process.*, 2007, **90**, 3-7.

19. A. Tilocca and E. Fois, *J. Phys. Chem. C*, 2009, **113**, 8683-8687.

20. A. Doménech, M. T. Doménech-Carbó and M. L. Vázquez de Agredos Pascual, *J. Phys. Chem. C*, 2007, **111**, 4585-4595.

21. F. Giulieri, S. Ovarlez and A. M. Chaze, Int. J. of Nanotechnol., 2012, **9**, 605-617.

22. R. Giustetto, O. Wahyudi, I. Corazzari and F. Turci, *Appl. Clay Sci.*, 2011, **52**, 41-50.

23. R. Giustetto, K. Seenivasan, F. Bonino, G. Ricchiardi, S. Bordiga, M. R. Chierotti and R. Gobetto, *J. Phys. Chem. C.*, 2011, **115**, 16764-16776.

24. S. Kowalak and A. Zywert, Clay Miner., 2011, **46**, 197-204.

25. C. Dejoie, P. Martinetto, E. Dooryhée, P. Strobel, S. Blanc, P. Bordat, R. Brown, F. Porcher, M. Sánchez del Río and M. Anne, *ACS Appl. Mater. Interfaces.*, 2010, **2**, 2308-2316.

26. X. Zhang, Z. Jin, Y. Li, S. Li and G. Lu, *J. Colloid Interface Sci.*, 2009, **333**, 285-293.

27. N. Yasarawan and J. S. van Duijneveldt, *Langmuir*, 2008, **24**, 7184-7192.

28. B. O'regan and M. Grfitzeli, *Nature*, 1991, **353**, 737-740.

29. I. Tomov, T. Dutton, B. VanWonterghem and P. Rentzepis, *J. Appl. Phys.*, 1991, **70**, 36-40.

30. K. Sasaki and T. Nagamura, *Appl. Phys. Lett.*, 1997, **71**, 434-436.

31. R. L. Frost, O. B. Locos, H. Ruan and J. T. Kloprogge, *Vib. Spectrosc.*, 2001, **27**, 1-13.

32. S. Weng, *Fourier Transform Infrared Spectroscopy*, Chemical Industry Press, Beijing, 2010.

33. A. Doménech, M. T. Doménech-Carbo and M. L. Vazquez de Agredos-Pascual, *Angew. Chem., Int. Ed.*, 2011, **50**, 5741-5744.

34. M. Bacci, *UV-VIS-NIR, FT-IR, and FORS spectroscopies. In Modern analytical methods in art and archaeology*, John Wiley &Sons, New York, 2000.

35. R. Rondao, J. S. r. Seixas de Melo, V. D. Bonifácio and M. J. Melo, *J. Phys. Chem. A*, 2010, **114**, 1699-1708.

36. M. Leona, F. Casadio, M. Bacci and M. Picollo, *J. Am. Ins. Conserv.*, 2004, **43**, 39-54.

37. R. L. Frost, G. A. Cash and J. T. Kloprogge, *Vib. Spectrosc.*, 1998, **16**, 173-184.
38. M. Augsburger, E. Strasser, E. Perino, R. Mercader and J. Pedregosa, *J. Phys. Chem. Solids.*, 1998, **59**, 175-180.
39. V. Gionis, *Am. Mineral.*, 2006, **91**, 1125-1133.
40. K. Witke, K.-W. Brzezinka and I. Lamprecht, *J. Mol. Struct.*, 2003, **661-662**, 235-238.
41. V. Vágvölgyi, L. M. Daniel, C. Pinto, J. Kristóf, R. L. Frost and E. Horváth, *J. Therm. Anal. Calorim.*, 2008, **92**, 589-594.

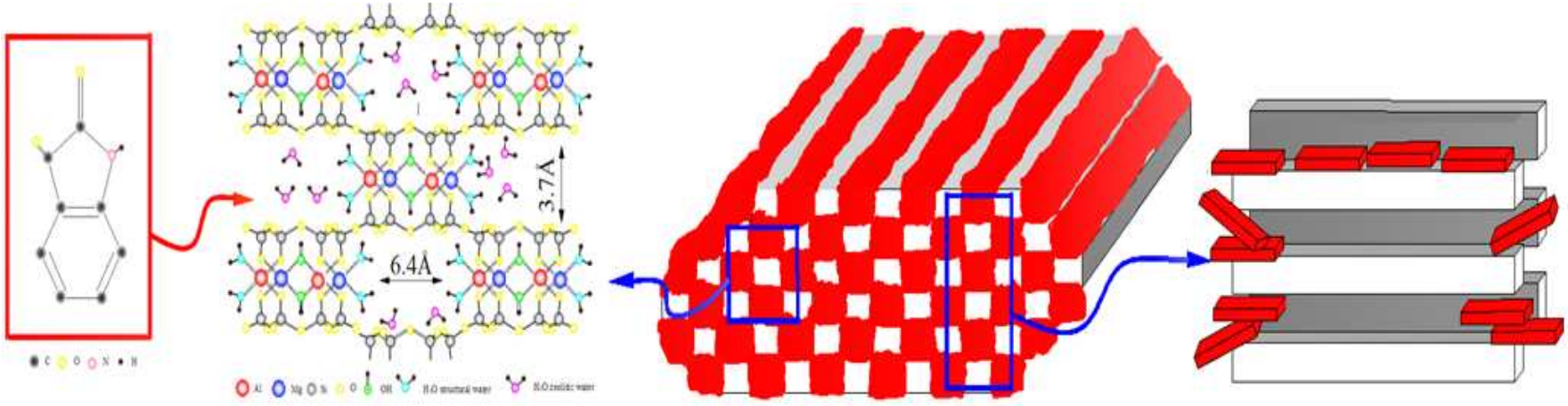

Heat treatment drove isatin inserted into the nanostructure of palygorskite, which endow the hybrid with good stability.